CORRELATIONS BETWEEN ANISOTROPY FLOW AND MEAN TRANSVERSE MOMENTUM USING SUBEVENT CUMULANTS IN SMALL SYSTEMS AT CMS

Rohit Kumar Singh
(IIT Madras)
for the CMS Collaboration

Nov 8, 2023

WPCF 2023 - XVI Workshop on Particle Correlations and Femtoscopy & IV Resonance Workshop 2023

Introduction

In heavy ion collisions:

- Anisotropic flow in the final state arises from the hydrodynamic response to the initial geometric anisotropy
- Mean p_T ($[p_T]$) reflects the strength of radial flow push, which is related to the initial energy density of the fireball
- The correlations between v_n and $[p_T]$ probe the fluctuations present in the initial density profile

$$\rho(v_n^2, [p_\mathrm{T}]) = \frac{\mathrm{cov}(v_n^2, [p_\mathrm{T}])}{\sqrt{\mathrm{var}(v_n^2)}\sqrt{\mathrm{var}([p_\mathrm{T}])}}$$

Introduction

In heavy ion collisions:

- Anisotropic flow in the final state arises from the hydrodynamic response to the initial geometric anisotropy
- Mean p_T ($[p_T]$) reflects the strength of radial flow push, which is related to the initial energy density of the fireball
- The correlations between v_n and $[p_T]$ probe the fluctuations present in the initial density profile

$$\rho(v_n^2, [p_T]) = \frac{\mathrm{cov}(v_n^2, [p_T])}{\sqrt{\mathrm{var}(v_n^2)}\sqrt{\mathrm{var}([p_T])}}$$

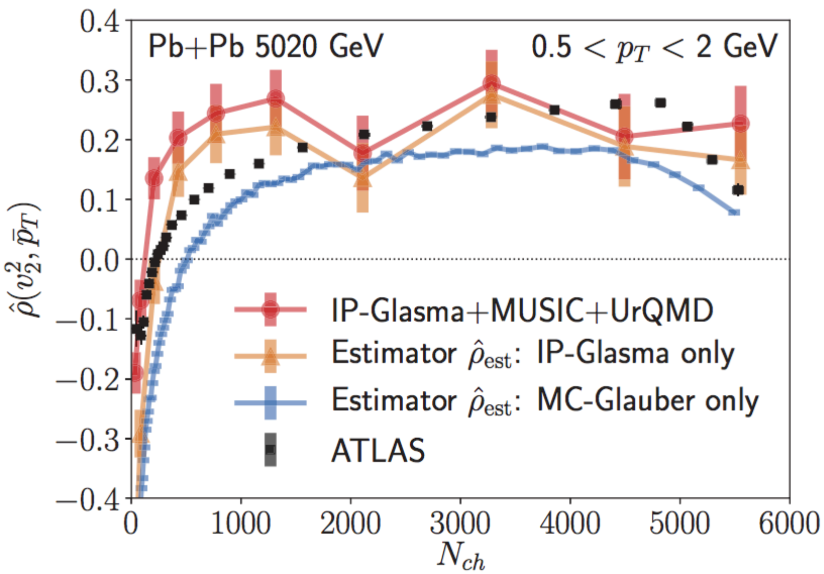

Phys. Rev. C 102, 034905 (2020)

Sensitive to the degree of sub-nucleon fluctuations

Introduction

In heavy ion collisions:

• Anisotropic flow in the final state arises from the hydrodynamic response to the initial geometric anisotropy

• Mean p_T ($[p_T]$) reflects the strength of radial flow push, which is related to the initial energy density of the fireball

• The correlations between v_n and $[p_T]$ probe the fluctuations present in the initial density profile

$$\rho(v_n^2, [p_T]) = \frac{\mathrm{cov}(v_n^2, [p_T])}{\sqrt{\mathrm{var}(v_n^2)}\sqrt{\mathrm{var}([p_T])}}$$

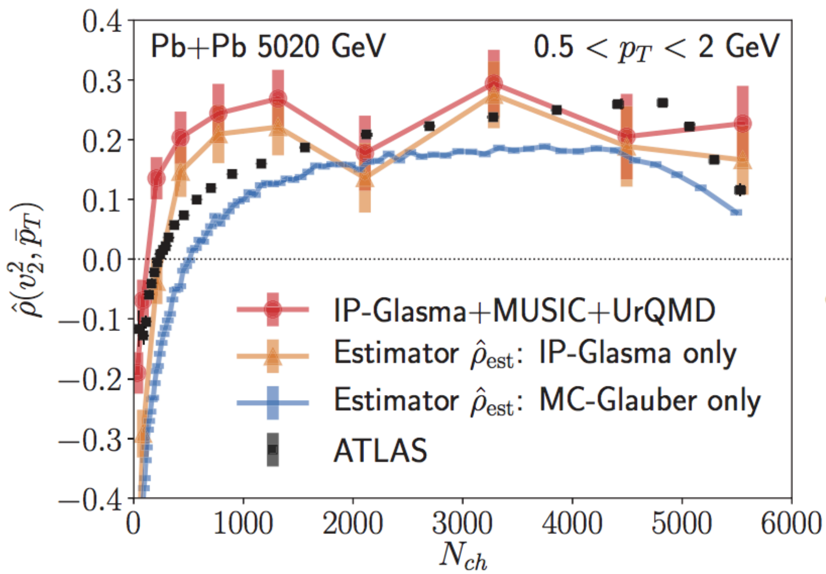

Phys. Rev. C 102, 034905 (2020)

Sensitive to the degree of sub-nucleon fluctuations

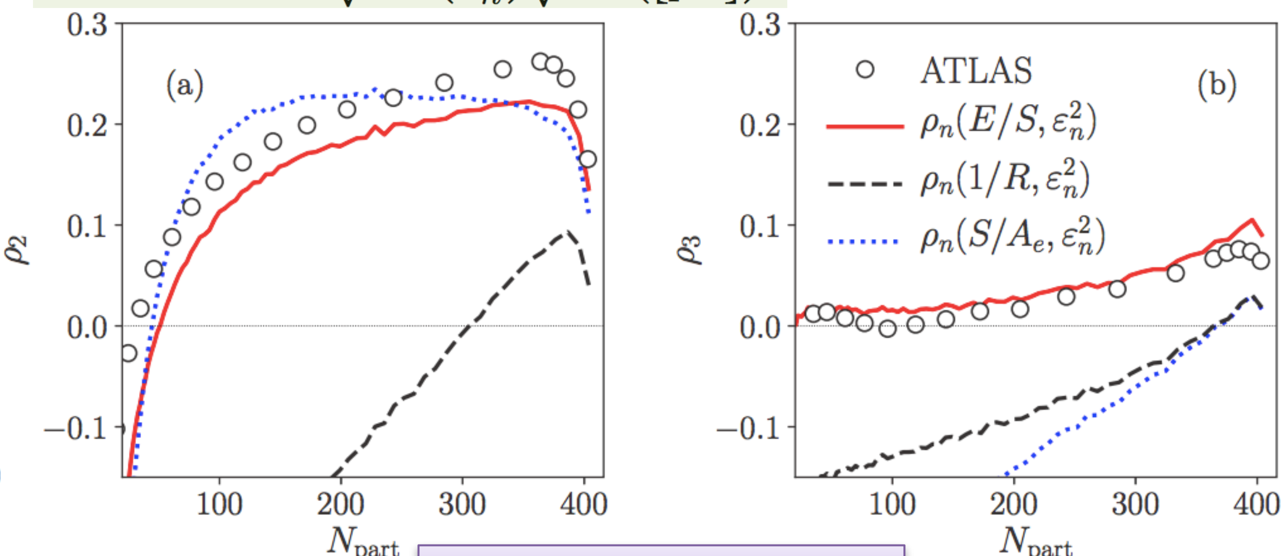

Phys. Rev. C 103, 024909 (2021)

The mechanism driving the correlations can be traced back to the initial density profile

Motivations for small systems (1)

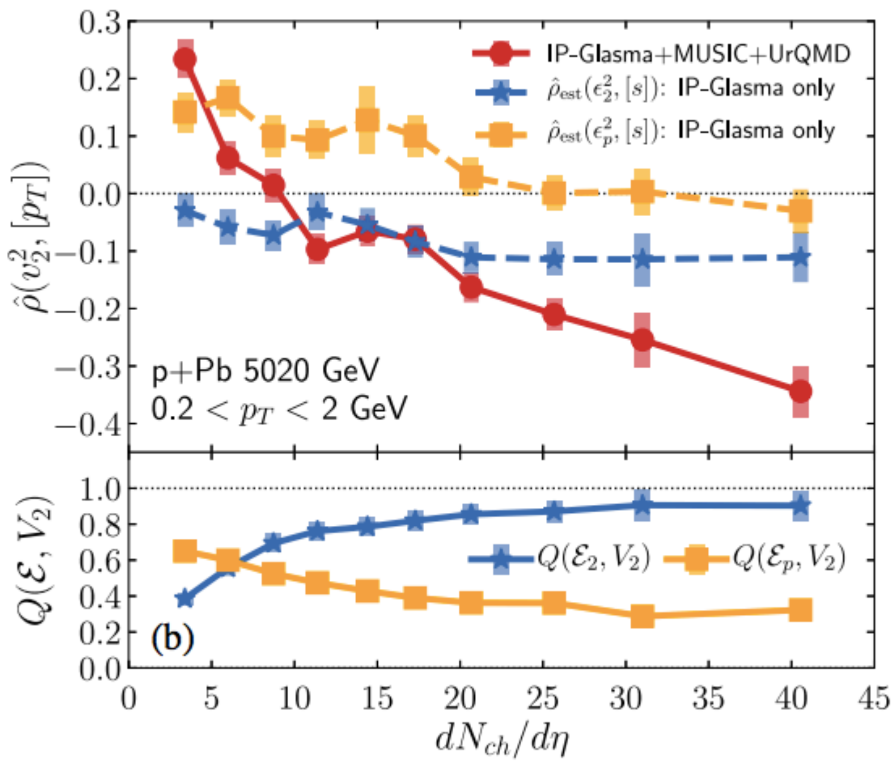

Phys. Rev. Lett. 125, 192301 (2020)

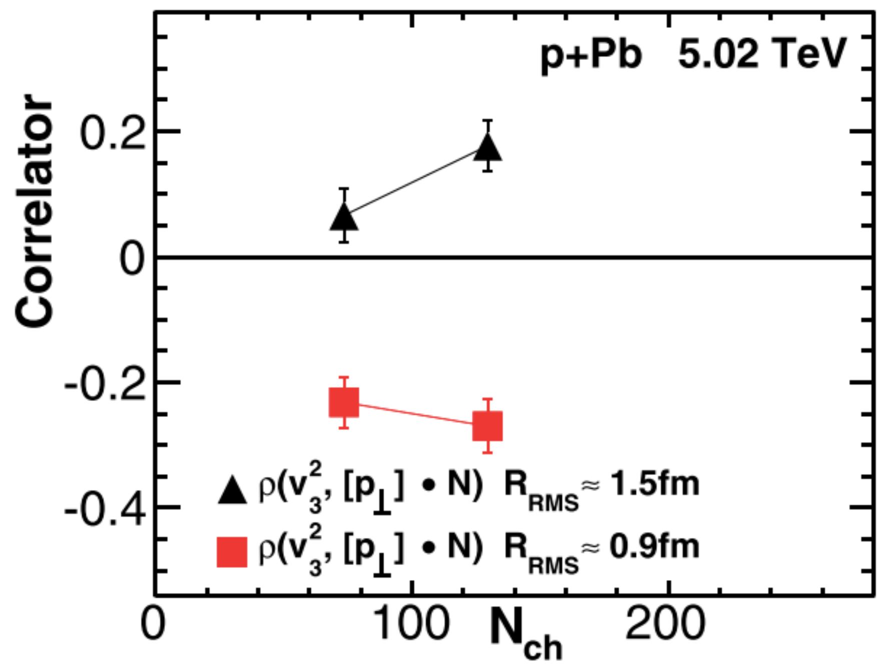

Phys. Rev. C 101, 064902 (2020)

- $\hat{\rho}$ exihibit a sign change with increasing multiplicity when an initial momentum anisotropy is present
- Carries information about the origin of the observed momentum anisotropy
- Sensitive to the transverse size of the initial fireball

Motivations for small systems (2)

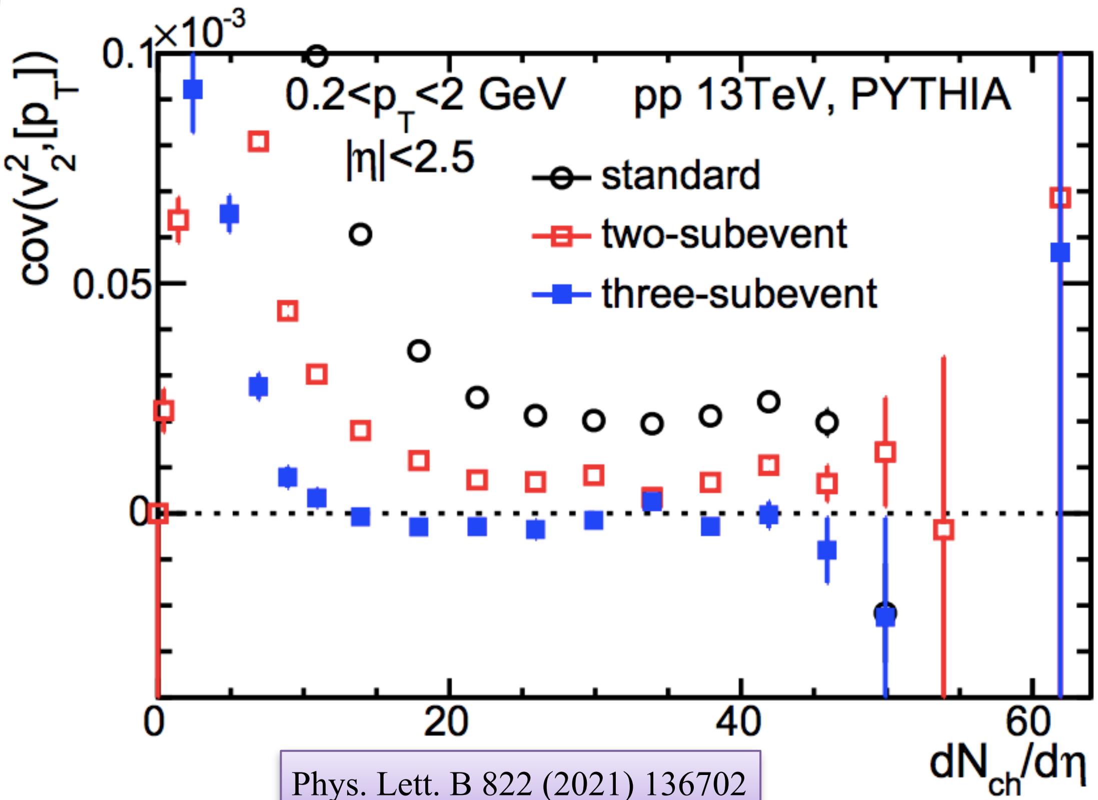

Phys. Lett. B 822 (2021) 136702

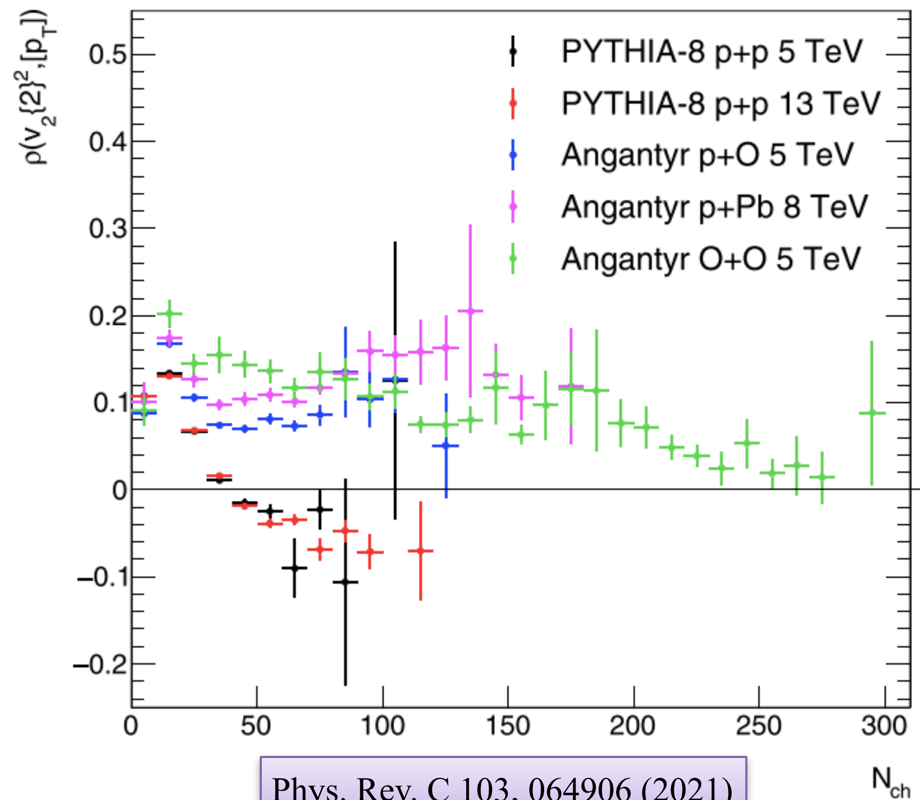

Phys. Rev. C 103, 064906 (2021)

- However, the correlations from PYTHIA alone have a sign change
- Nonflow has to be carefully dealt
- The goal of this analysis:
  - Introduce a new variable to remove more nonflow
  - Search for sign change at the lowest possible multiplicity in pp/pPb/PbPb collisions

Analysis Method (1)

$$\rho(v_2^2, [p_\mathrm{T}]) = \frac{\mathrm{cov}(v_2^2, [p_\mathrm{T}])}{\sqrt{\mathrm{Var}(v_2^2)_{dyn}}\sqrt{\mathrm{Var}([p_\mathrm{T}])_{dyn}}} \quad (1)$$

$$\rho(c_2\{2\}, [p_\mathrm{T}])$$

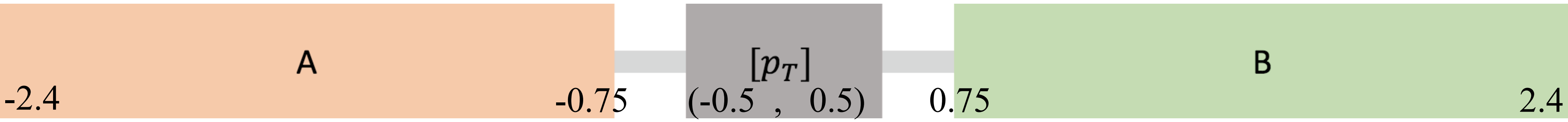

Subevents A and B are used for calculation of $c_2\{2\}$; $|\eta|<0.5$ for $[p_\mathrm{T}]$

Analysis Method (1)

$$\rho(v_2^2, [p_\mathrm{T}]) = \frac{\mathrm{cov}(v_2^2, [p_\mathrm{T}])}{\sqrt{\mathrm{Var}(v_2^2)_{dyn}}\sqrt{\mathrm{Var}([p_\mathrm{T}])_{dyn}}} \quad (1)$$

$$\rho(c_2\{2\}, [p_\mathrm{T}])$$

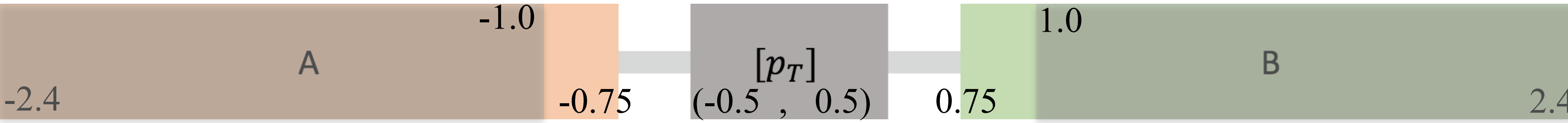

Subevents A and B are used for calculation of $c_2\{2\}$; $|\eta|<0.5$ for $[p_\mathrm{T}]$

Covariance between $c_2\{2\}$ and $[p_\mathrm{T}]$:

$$\mathrm{cov}(c_2\{2\}, [p_\mathrm{T}]) = \Re\mathfrak{e}\left\langle \sum_{a,b} \exp^{2i(\phi_a - \phi_b)} \left([p_\mathrm{T}] - \langle [p_\mathrm{T}] \rangle\right) \right\rangle \quad (2)$$

Dynamic variance of $c_2\{2\}$:

$$\mathrm{Var}(c_2\{2\})_{\mathrm{dyn}} = \langle\langle 4\rangle\rangle - \langle\langle 2\rangle\rangle^2 \quad (3)$$

Variance of $[p_\mathrm{T}]$ from dynamic $[p_\mathrm{T}]$ fluctuation c_k:

$$c_k = \left\langle \left[(p_{\mathrm{T}i} - \langle [p_\mathrm{T}] \rangle)(p_{\mathrm{T}j} - \langle [p_\mathrm{T}] \rangle) \right] \right\rangle \quad (4)$$

Analysis Method (2)

$$\rho(v_2^2, [p_\mathrm{T}]) = \frac{\mathrm{cov}(v_2^2, [p_\mathrm{T}])}{\sqrt{\mathrm{Var}(v_2^2)_{dyn}}\sqrt{\mathrm{Var}([p_\mathrm{T}])_{dyn}}} \quad (1)$$

Extend and study the new variable to remove more nonflow

$$\rho(c_2\{2\}, [p_\mathrm{T}]) \rightarrow \rho(c_2\{4\}, [p_\mathrm{T}])$$

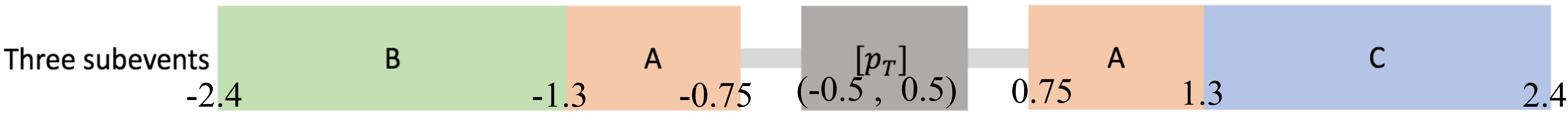

$c_2\{4\}$ is analyzed with three subevent method

$$c_2\{4\}_{3\text{-sub}} = \langle 4\rangle_{a,a|b,c} - 2\langle 2\rangle_{a|b}\langle 2\rangle_{a|c}$$

Phys. Rev. C 96, 034906 (2017)

Observables in this analysis

- This analysis focuses on small systems
- It is the first paper to :
  - use multiparticle correlations for flow when correlating with $[p_T]$
  - explore the correlator with different η gaps to study nonflow effects
  - measure v_3 - $[p_T]$ correlations in small systems
  - include measurements in pp collisions

Results

Results are presented as a function of N_{ch}, which is defined in $0.5<p_T<5.0$ GeV, $|\eta|<2.4$, and corrected for tracking efficiency

CMS-PAS-HIN-21-012 (link)

Results for covariance

CMS-PAS-HIN-21-012

n=2

n=3

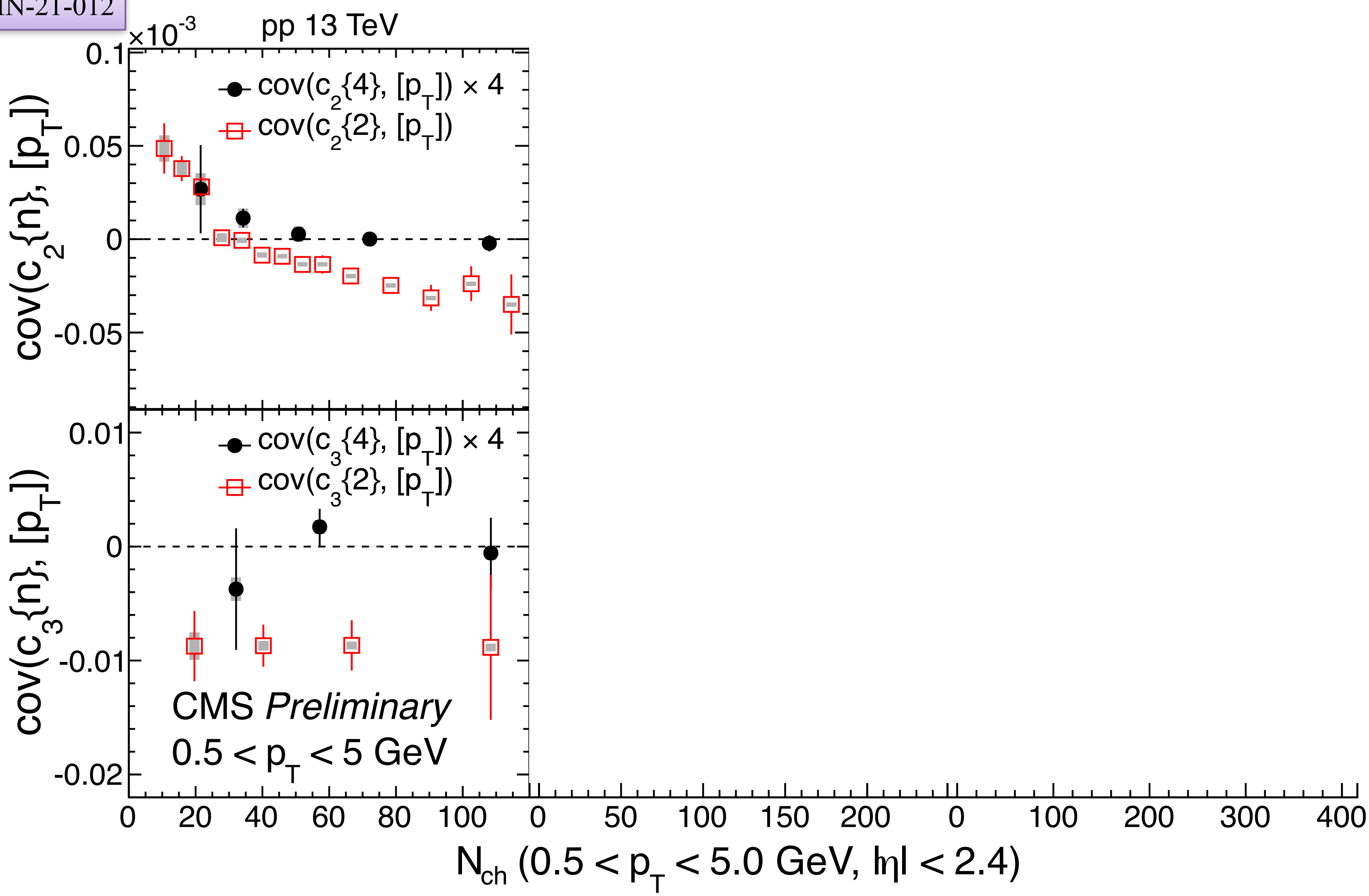

- Clear sign change for pp collisions with $c_2\{2\}$
- No sign change at low N_{ch} using multiparticle correlations with current statistics
- The sign of the normalized correlator is determined by the covariance

Results for **covariance**

CMS-PAS-HIN-21-012

n=2

n=3

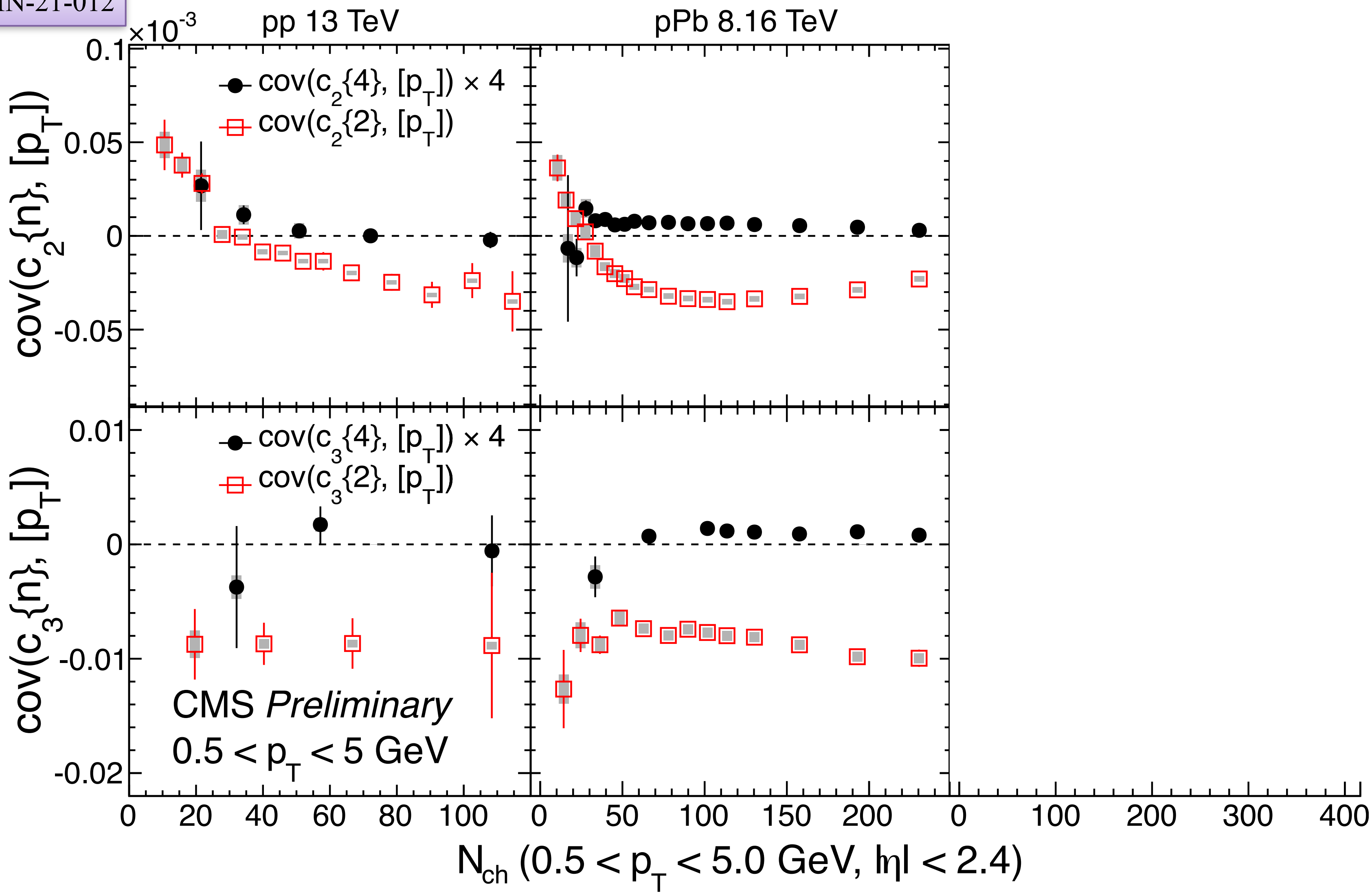

- Clear sign change for pp and pPb collisions with $c_2\{2\}$
- No sign change at low N_{ch} using multiparticle correlations with current statistics
- The sign of the normalized correlator is determined by the covariance

Results for **covariance**

CMS-PAS-HIN-21-012

n=2

n=3

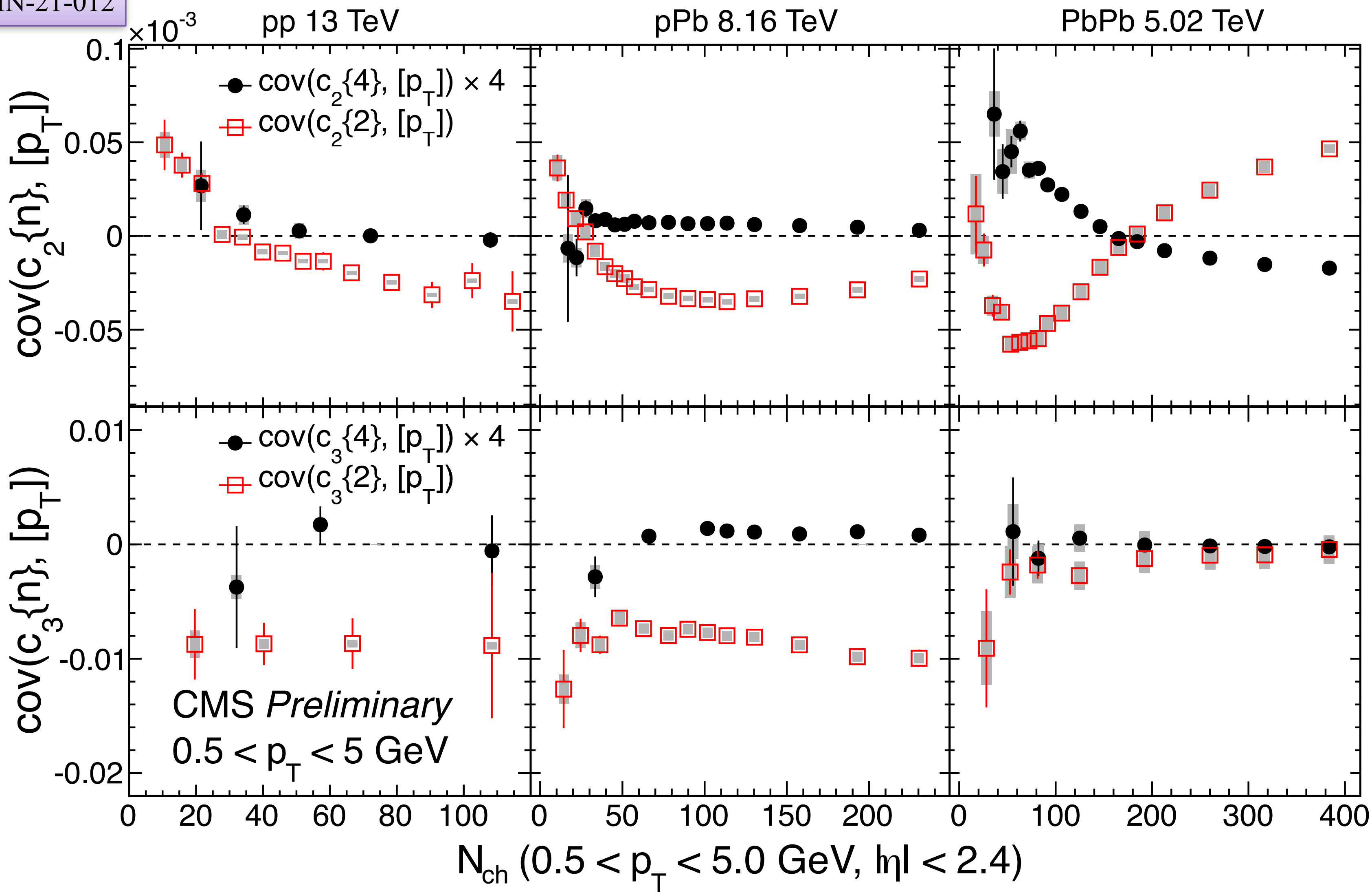

- Clear sign change for pp and pPb collisions with $c_2\{2\}$
- No sign change at low N_{ch} using multiparticle correlations with current statistics
- The sign of the normalized correlator is determined by the covariance

Results for the correlator

CMS-PAS-HIN-21-012

n=2

n=3

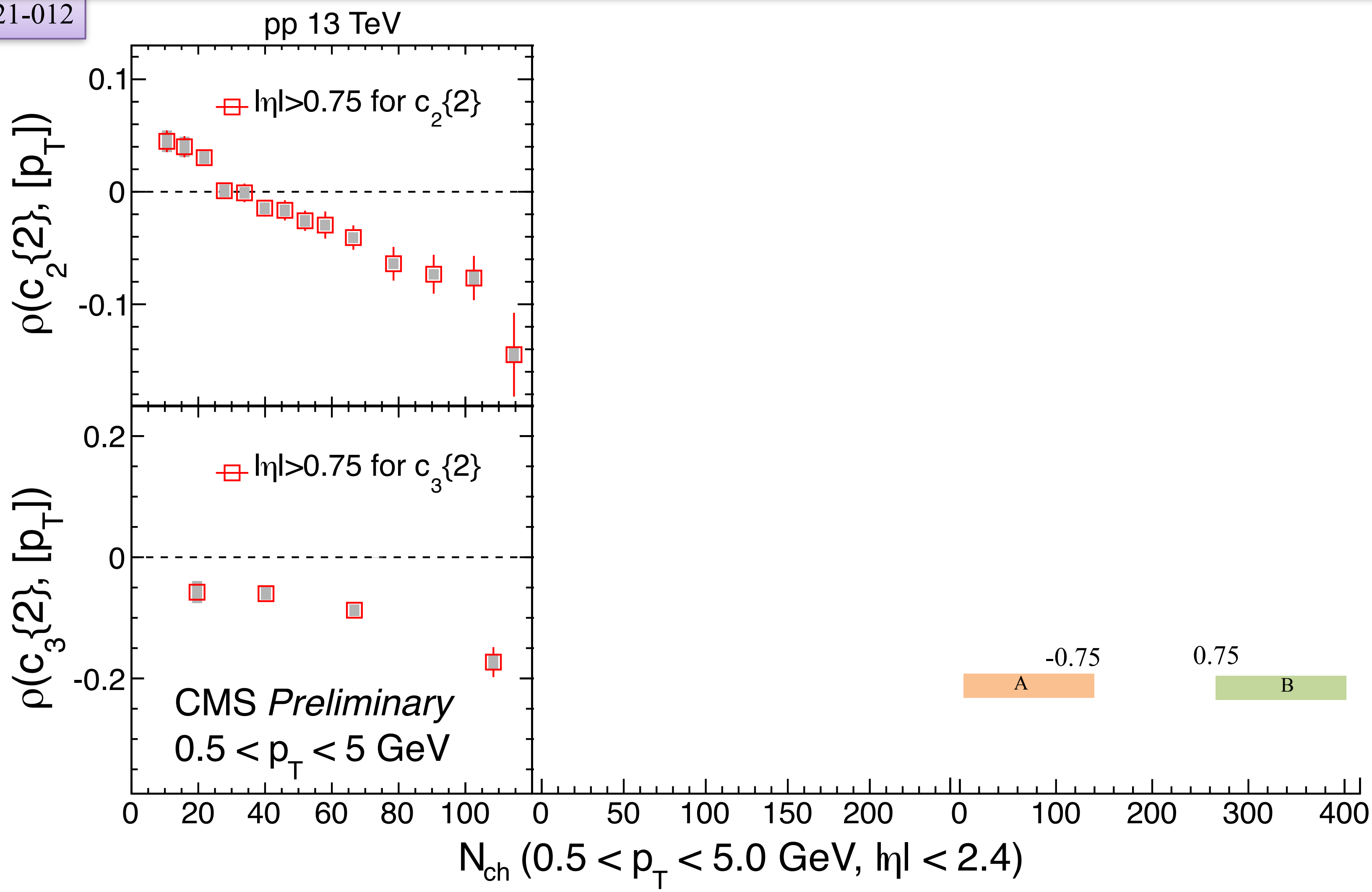

- Apparent sign change for $\rho(c_2\{2\}, [p_T])$ in pp collisions

Results for the correlator

CMS-PAS-HIN-21-012

n=2

n=3

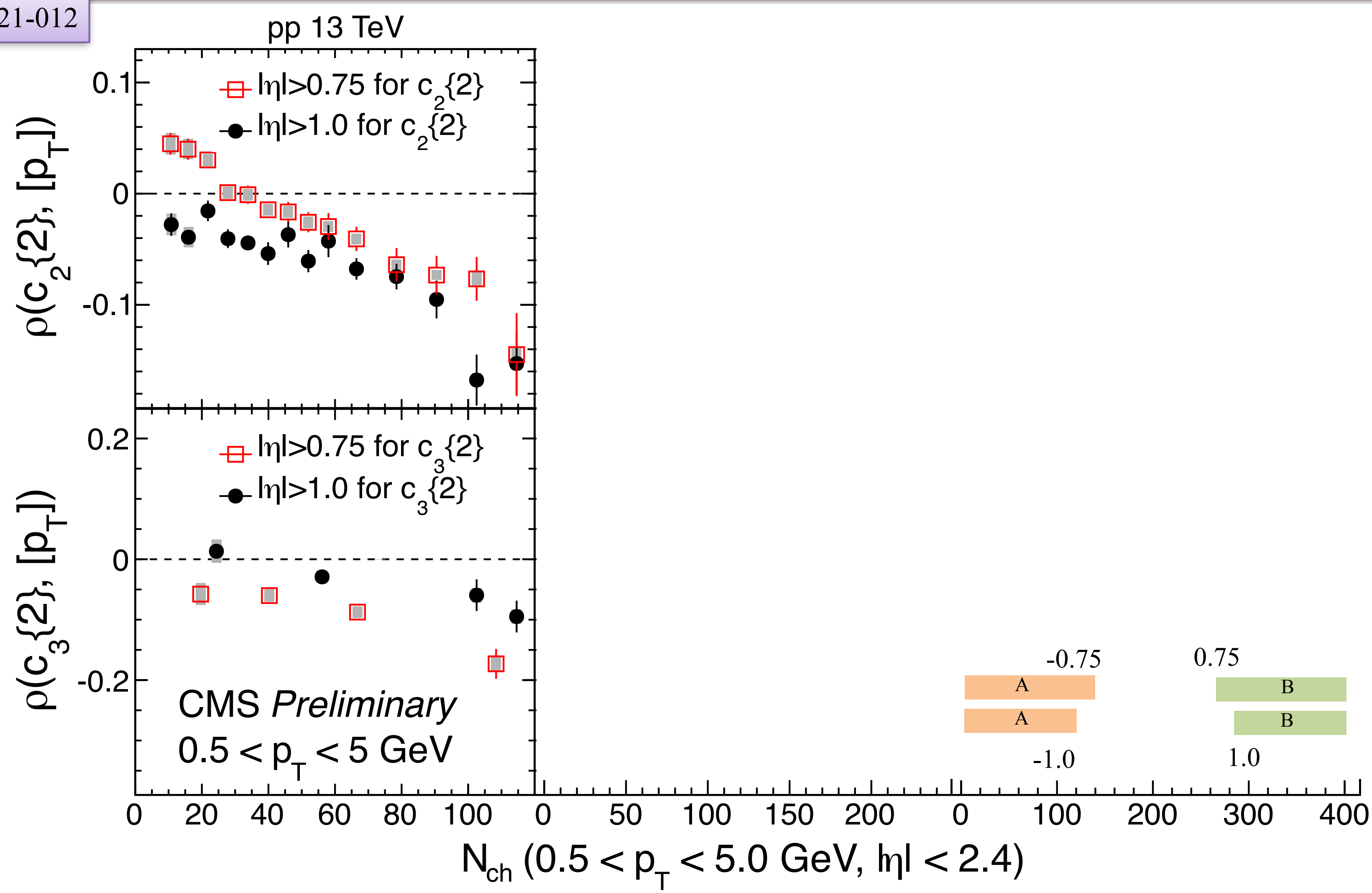

- Apparent sign change for $\rho(c_2\{2\}, [p_T])$ in pp collisions
- However, no sign change is observed when using $|\eta|>1.0$ for $c_2\{2\}$

Results for the correlator

CMS-PAS-HIN-21-012

n=2

n=3

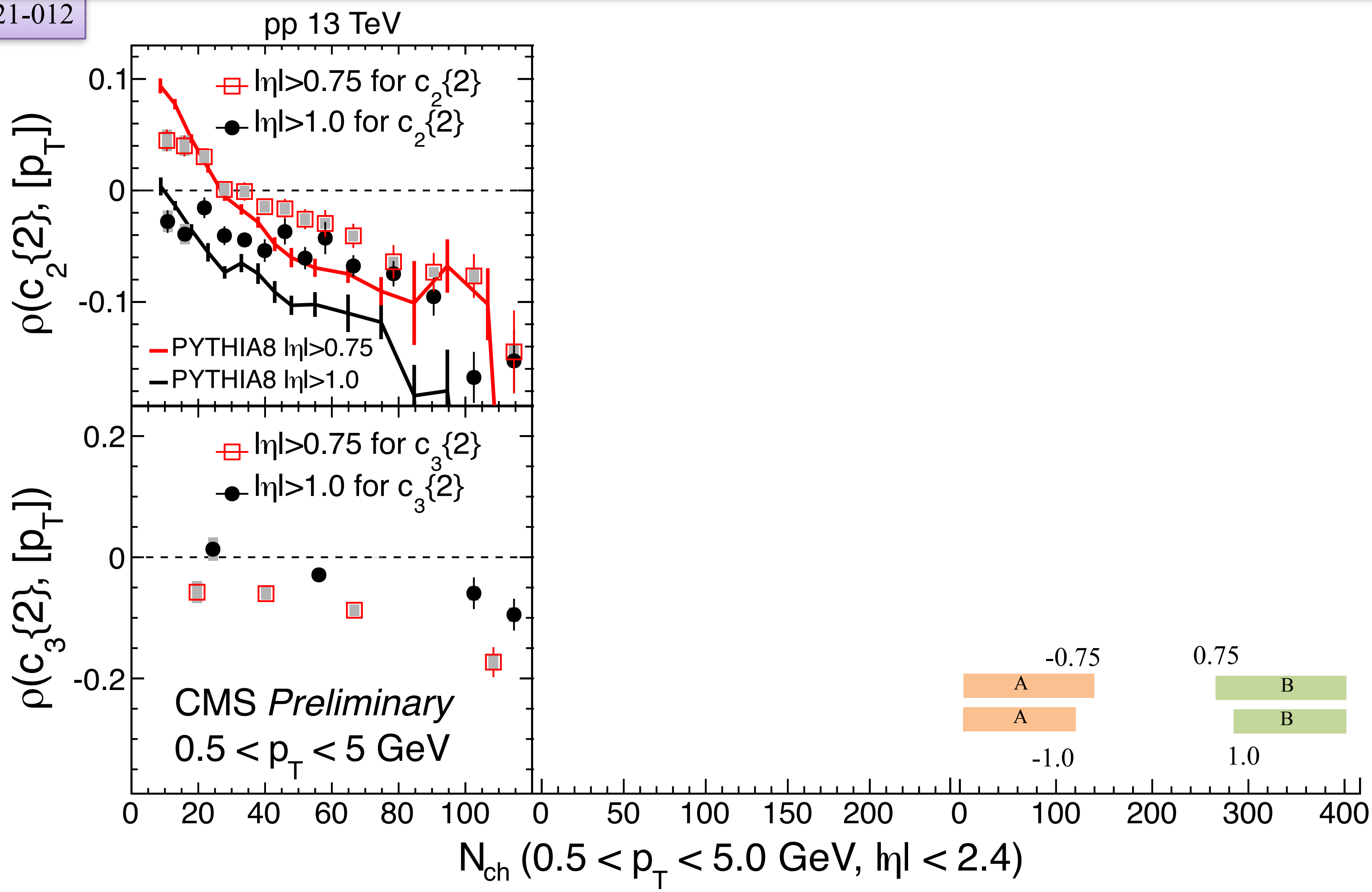

- Apparent sign change for $\rho(c_2\{2\}, [p_T])$ in pp collisions
- However, no sign change is observed when using $|\eta|>1.0$ for $c_2\{2\}$
- Also true for PYTHIA8 events

Results for the correlator

CMS-PAS-HIN-21-012

n=2

n=3

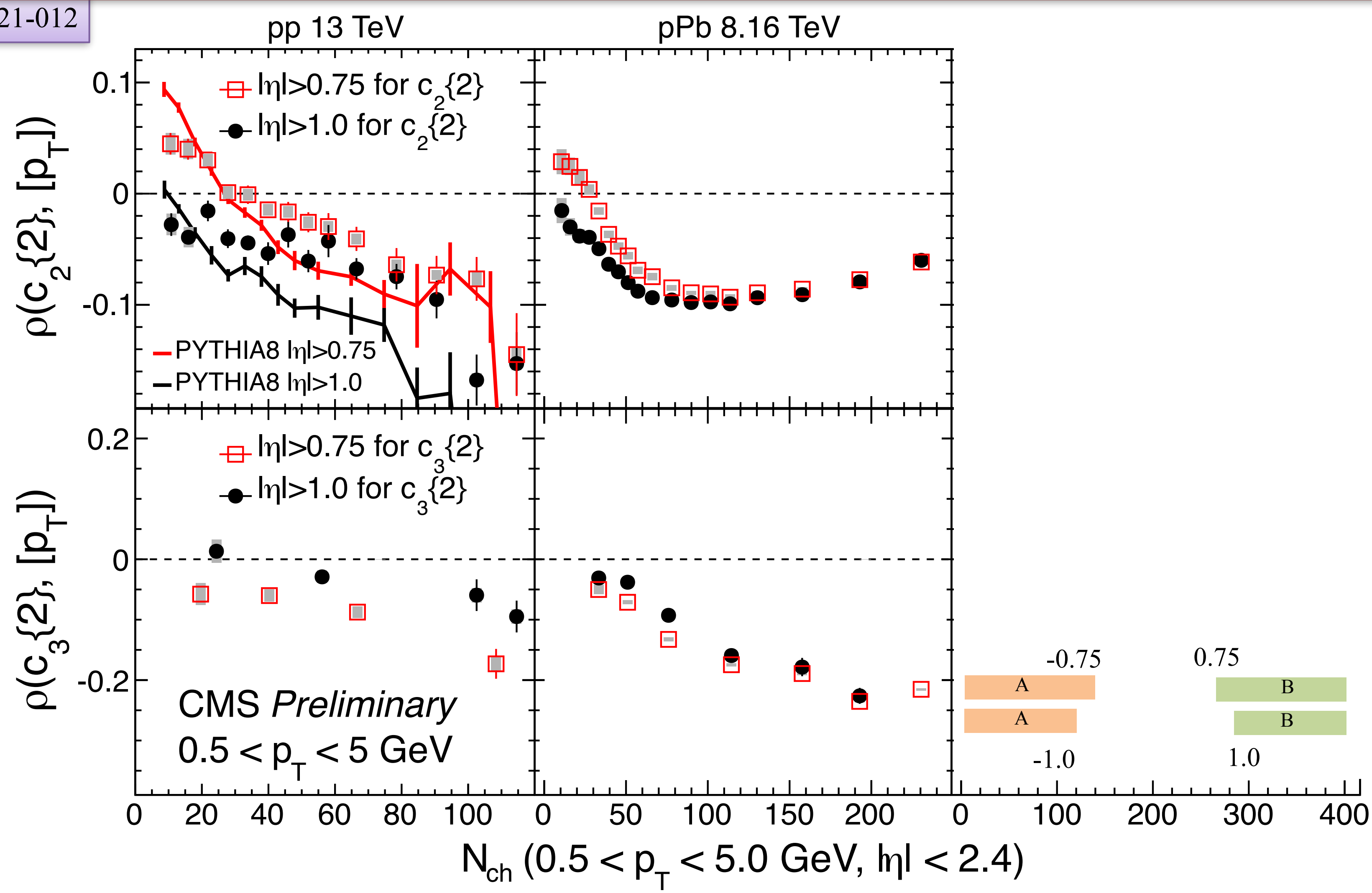

- Apparent sign change for $\rho(c_2\{2\}, [p_T])$ in pPb -> agree with IP-Glasma+hydro
- However, no sign change is observed when using $|\eta|>1.0$ for $c_2\{2\}$

Results for the correlator

CMS-PAS-HIN-21-012

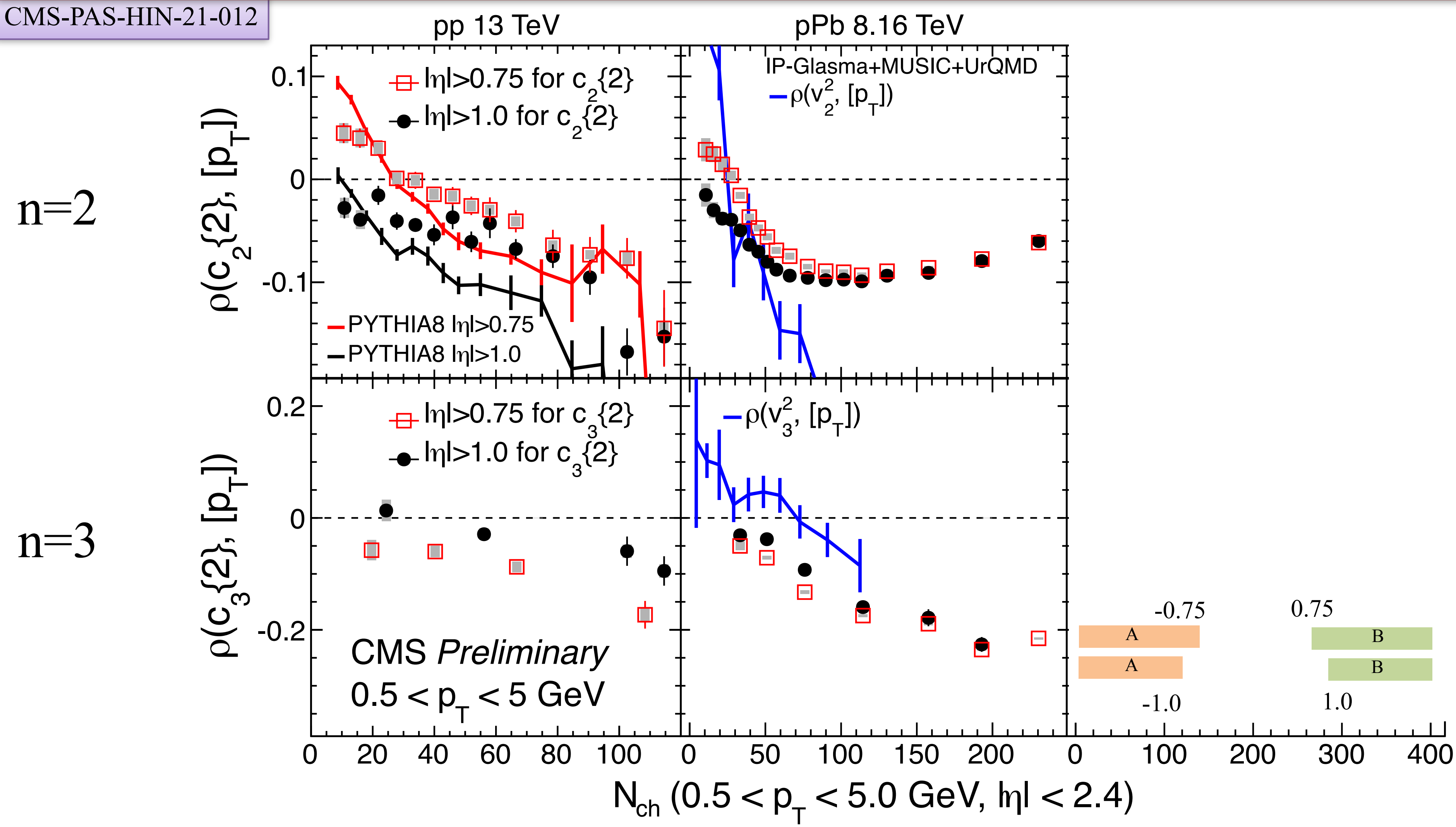

- Apparent sign change for $\rho(c_2\{2\}, [p_T])$ in pPb -> agree with IP-Glasma+hydro
- However, no sign change is observed when using $|\eta|>1.0$ for $c_2\{2\}$
- After removing nonflow with larger η gap, no evidence of CGC in data

Results for the correlator

CMS-PAS-HIN-21-012

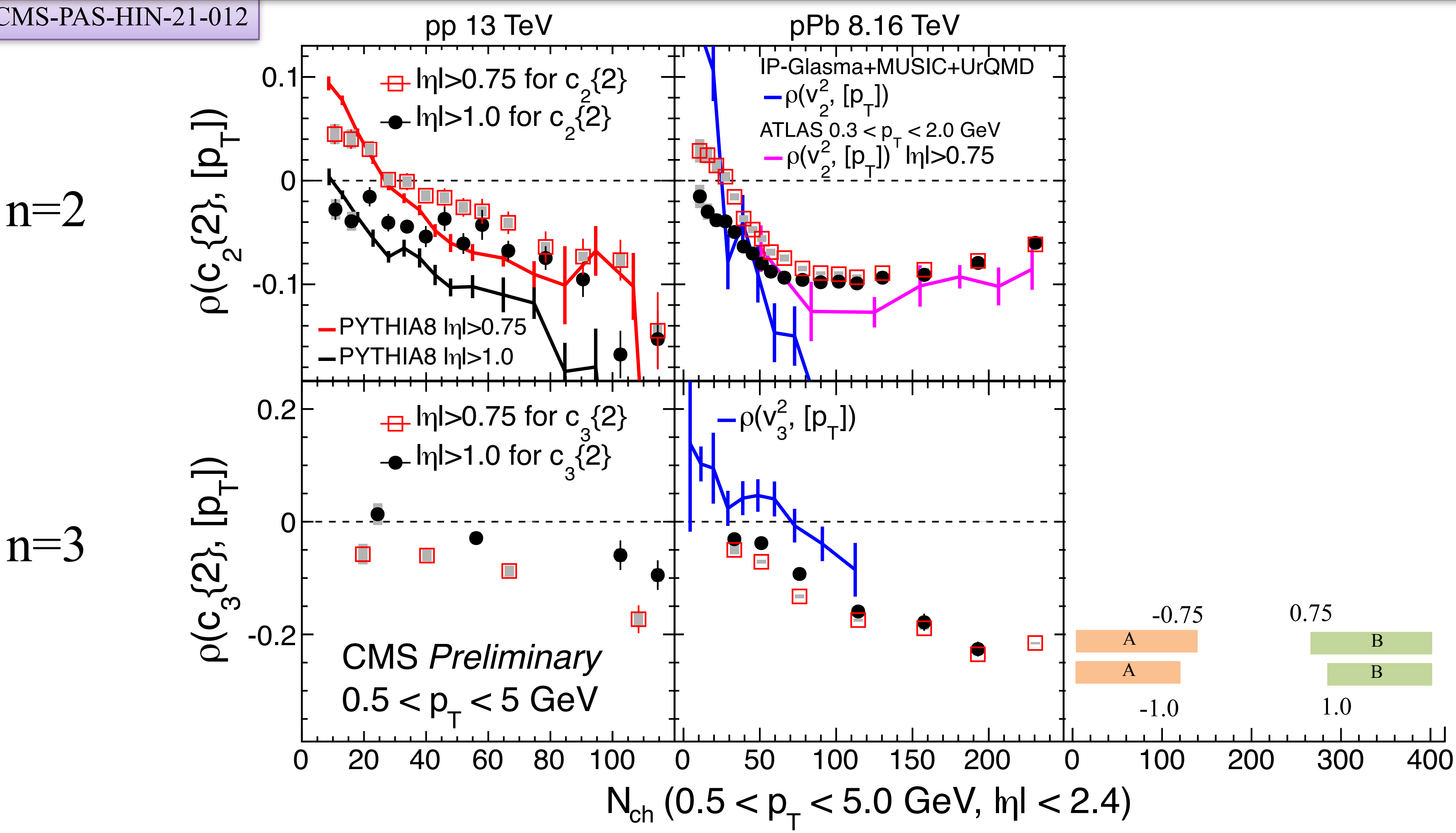

- Apparent sign change for $\rho(c_2\{2\}, [p_T])$ in pPb -> agree with IP-Glasma+hydro
- However, no sign change is observed when using $|\eta|>1.0$ for $c_2\{2\}$
- After removing nonflow with larger η gap, no evidence of CGC in data

Results for the correlator

CMS-PAS-HIN-21-012

n=2

n=3

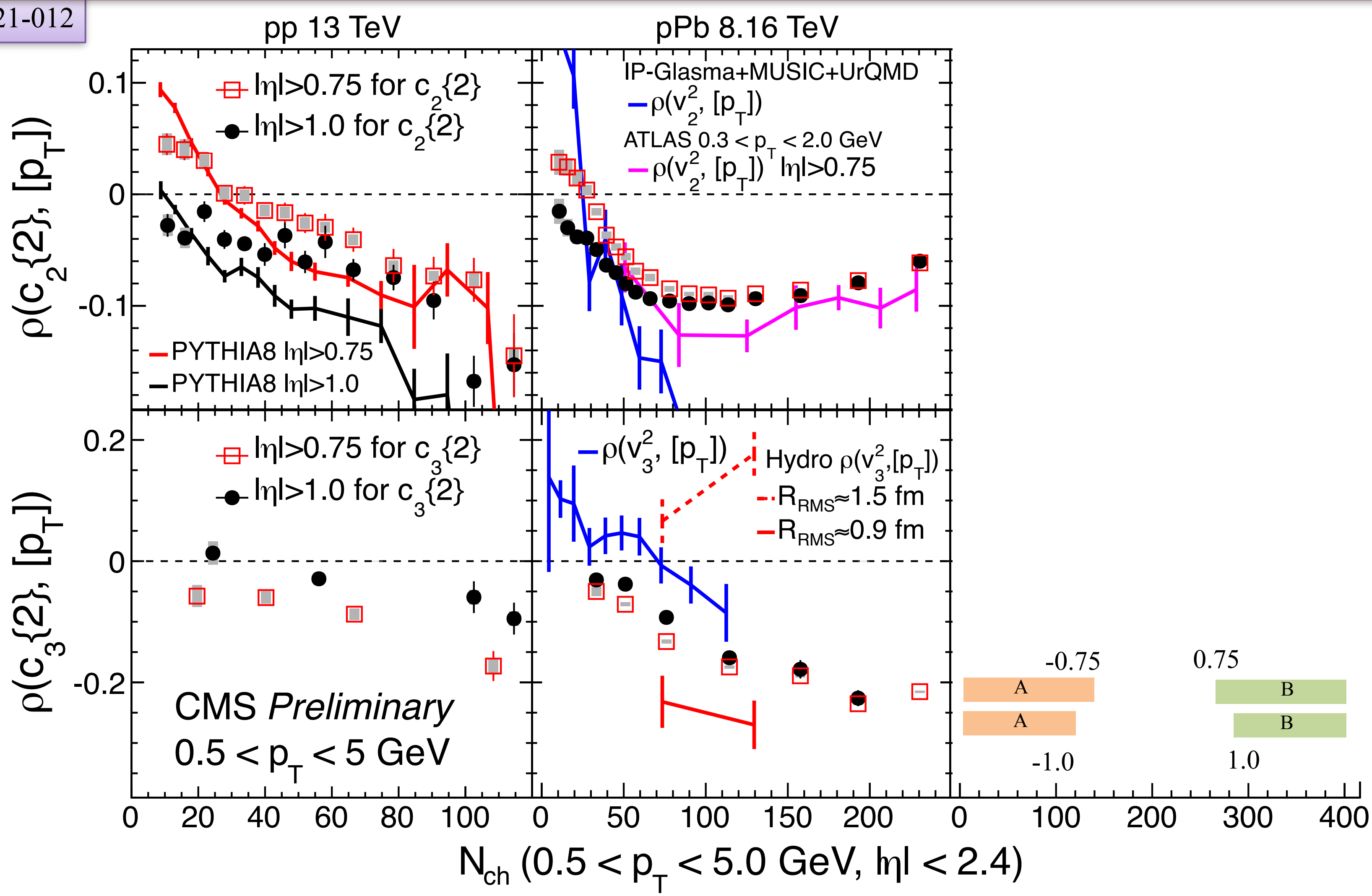

- Apparent sign change for $\rho(c_2\{2\}, [p_T])$ in pPb -> agree with IP-Glasma+hydro
- However, no sign change is observed when using $|\eta|>1.0$ for $c_2\{2\}$
- After removing nonflow with larger η gap, no evidence of CGC in data
- Data better described by the smaller initial fireball $R_{RMS}=0.9$ fm in hydro

Results for the **correlator**

CMS-PAS-HIN-21-012

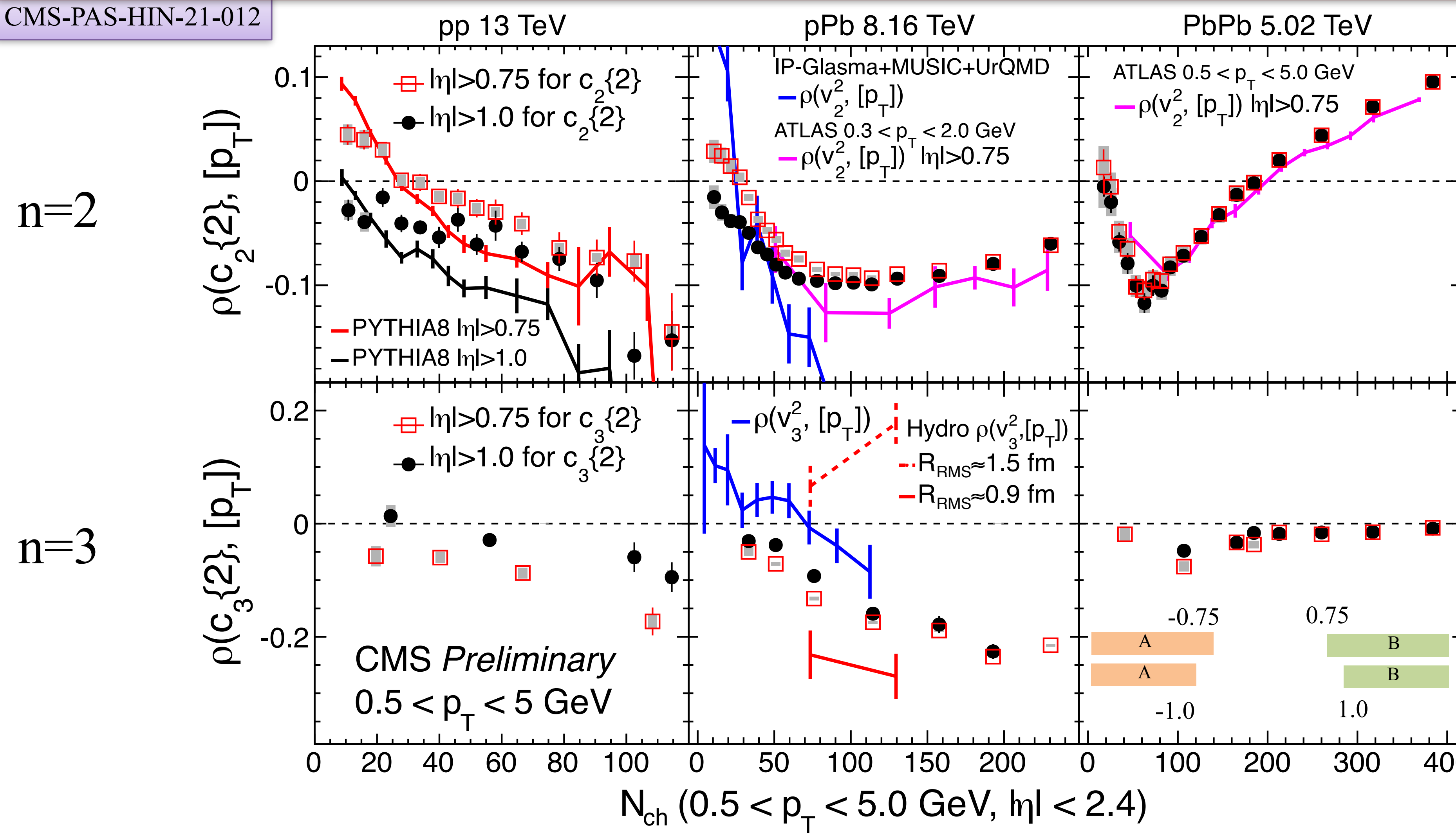

- Apparent sign change for $\rho(c_2\{2\}, [p_T])$ in pPb -> agree with IP-Glasma+hydro
- However, no sign change is observed when using $|\eta|>1.0$ for $c_2\{2\}$
- After removing nonflow with larger η gap, no evidence of CGC in data
- Data better described by the smaller initial fireball $R_{RMS}=0.9$ fm in hydro

Summary

- The correlations between $[p_T]$ and cumulants from both two- and four-particle correlations in small systems are presented
- Apparent sign change is observed for $\rho(c_2\{2\}, [p_T])$ in pp and pPb
- However, no sign change is observed with larger η gap in $c_2\{2\}$
  - ATLAS default is $|\eta|>0.75$, with $|\Delta\eta|>1.5$
  - ALICE default is $|\eta|>0.4$, with $|\Delta\eta|>0.8$
  - CMS is studying both $|\eta|>0.75$ ($|\Delta\eta|>1.5$) and $|\eta|>1.0$ ($|\Delta\eta|>2.0$)
- After removing more nonflow with both two- and four-particle correlation cumulants, there is no evidence of CGC in data
- These high-precision data and the observables employing multiparticle correlations should provide new insight into the origin of azimuthal anisotropy in small collision systems

Backup

Dynamic flow fluctuations

Keeping $\mathrm{cov}(c_2\{4\}, [p_T])$ but drop $\rho(c_2\{4\}, [p_T])$ in this analysis

- The reason is we are not 100% sure if the variance $\mathrm{Var}(c_2\{4\})_{dyn}$ in our new method is truly dynamic
- It may contain statistical fluctuations in our current method
- The measurement of v_n fluctuation in small systems is a task our community has not accomplished. The event-by-event v_n studies all stopped at 60-70% centrality in AA collisions

Mapping between N_{ch} and $N_{trk}^{offline}$

Table 1: Average multiplicity of reconstructed tracks per N_{ch}^{rec} bin for N_{ch} and $N_{trk}^{offline}$ in pp, pPb, and PbPb collisions. Uncertainties for the tracking efficiency corrected N_{ch} are included.

	pp		pPb		PbPb	
N_{ch}^{rec} range	$\langle N_{ch} \rangle$	$\langle N_{trk}^{offline} \rangle$	$\langle N_{ch} \rangle$	$\langle N_{trk}^{offline} \rangle$	$\langle N_{ch} \rangle$	$\langle N_{trk}^{offline} \rangle$
$[0, 20)$	8 ± 0.3	9	11 ± 0.4	12	16 ± 0.6	14
$[20, 40)$	34 ± 1	34	36 ± 1	36	57 ± 2	48
$[40, 60)$	58 ± 2	56	60 ± 2	60	96 ± 4	80
$[60, 80)$	82 ± 3	78	83 ± 3	82	135 ± 5	112
$[80, 100)$	106 ± 4	101	107 ± 4	105	175 ± 7	144
$[100, 150)$	132 ± 5	125	140 ± 6	137	240 ± 10	197
$[150, 200)$			198 ± 8	191	335 ± 13	276
$[200, 250)$			256 ± 10	246	434 ± 17	353
$[250, 300)$					535 ± 21	426

Phys. Lett. B 718 (2013) 795

- The mapping table between N_{ch} and $N_{trk}^{offline}$

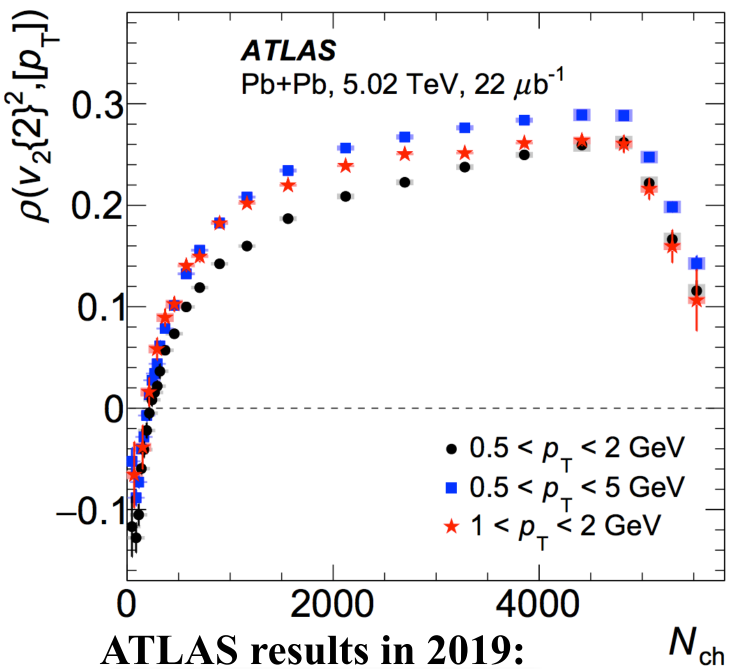

ATLAS results in 2019: Eur. Phys. J. C 79 (2019) 985

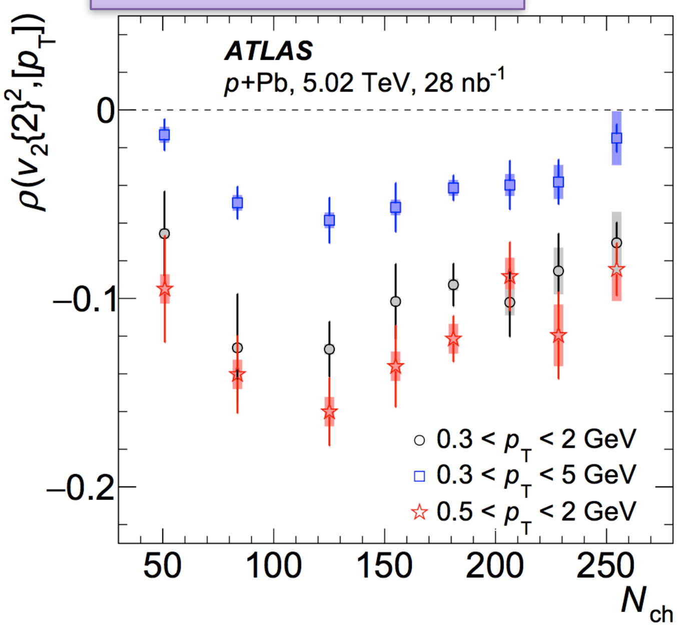

ALICE: Phys.Lett.B 834 (2022) 137393

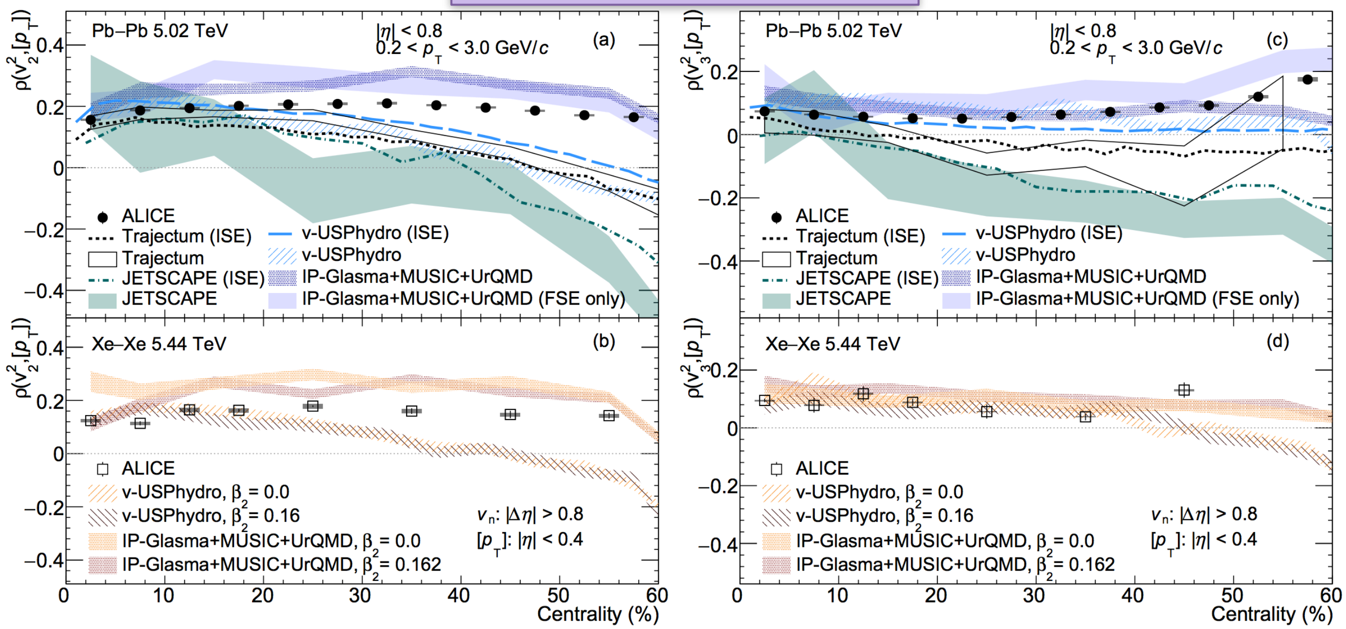

- ATLAS results in pPb, PbPb, and XeXe collisions
- ALICE results in PbPb and XeXe collisions
- Some recent studies from STAR